GL02301

DOE/ID/12079-7
ESL-40

DELINEATION OF AN ELECTRICAL RESISTIVITY ANOMALY, MALPAIS AREA, BEOWAWE KGRA, EUREKA AND LANDER COUNTIES, NEVADA

by

Christian Smith

July, 1980

EARTH SCIENCE LABORATORY DIVISION
UNIVERSITY OF UTAH RESEARCH INSTITUTE
420 Chipeta Way, Suite 120
Salt Lake City, Utah 84108

Prepared for the
DEPARTMENT OF ENERGY
DIVISION OF GEOTHERMAL ENERGY
Under Contract No. DE-AC07-80ID12079

CONTENTS

ILLUSTRATIONS

ABSTRACT

The Beowawe Geysers hydrothermal system discharges near the base of an east-west-trending Basin and Range fault approximately 50 km east of Battle Mountain, Nevada. The upthrown block south of The Geysers is called the Malpais. Exposures 2-3 km east of The Geysers reveal a segment of the eastern boundary of a major north-northwest-trending Miocene graben. The Geysers are located along the margin of the graben near its intersection with the Basin and Range fault.

A simple numerical model of previously released bipole-dipole resistivity data shows the margin of the graben to be anomalously conductive below the Malpais. The conductive area has been delineated with data from a dipole-dipole resistivity survey run in April, 1980 for this study. Detailed numerical models of these data define a 1250 m wide body with resistivities less than 20 ohm-m that appear to connect The Geysers and the graben boundary. The minimum depth to the conductor is interpreted to be 375 m; its depth extent is undetermined.

The electrical data do not resolve whether the anomaly below the Malpais may be the product of a defunct hydrothermal system or the signature of an active system. If thermal gradient data detect an enhanced heat flow anomaly in the same area, the Malpais may be a viable geothermal exploration target within the Beowawe KGRA.

INTRODUCTION

The Beowawe Geysers, 50 km east of Battle Mountain, Nevada (Figure 1), have formed a 2.0 sq km sinter terrace along a short segment of the base of the Malpais (Figure 2). Prior to 1979, most geophysical exploration for a geothermal resource suitable for electric power generation at Beowawe focused on the Whirlwind Valley north of the Malpais. The southern ends of four dipole-dipole resistivity lines centered in the Whirlwind Valley cross the Malpais where they suggest the location of a conductive anomaly (Smith, 1979). In support of the geothermal program and to understand better the geometry of the Malpais anomaly, three additional dipole-dipole lines perpendicular to structural trends were run for this study. This report presents numerical models of the new data and suggests that the conductive body below the Malpais may connect The Geysers to a deep-seated graben-margin fault zone.

This study will be incorporated into a comprehensive case study of the Beowawe area (Earth Science Laboratory, in preparation).

Geologic Setting

Figure 2 is a generalized geologic map from Struhsacker (1980) showing the structural patterns in the Malpais. The Geysers discharge along a segment of an east-west-trending Basin and Range fault; this segment is bounded by the North and South Cross-Faults of Osterling (1962). The major deep-seated structure in the Malpais is a north-northwest-trending fault set that formed the eastern boundary of a Miocene graben initially identified by Zoback (1978) and named the Dunphy Pass fault zone by Struhsacker (1980). The faults along

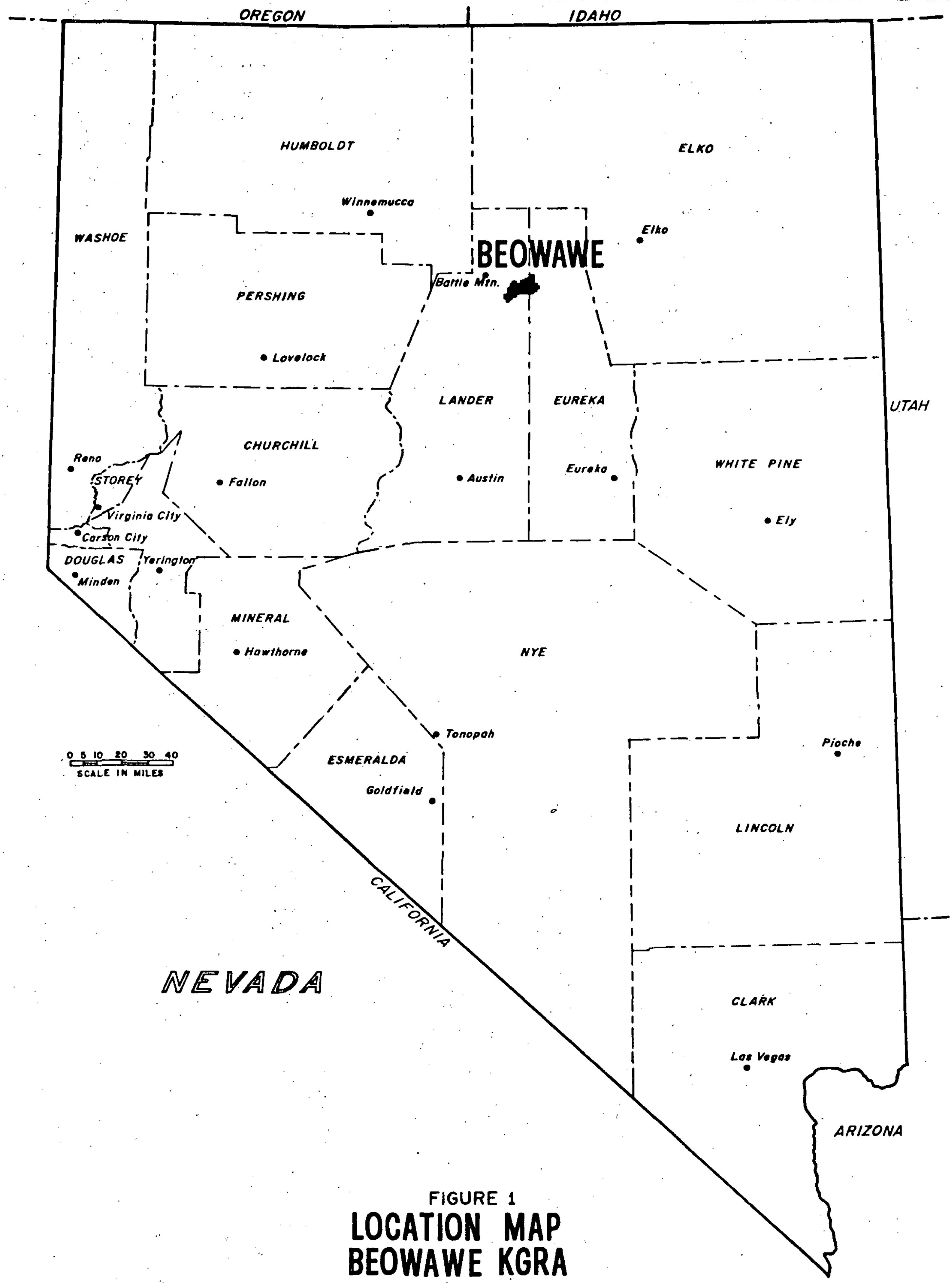

FIGURE 1
LOCATION MAP
BEOWAWE KGRA

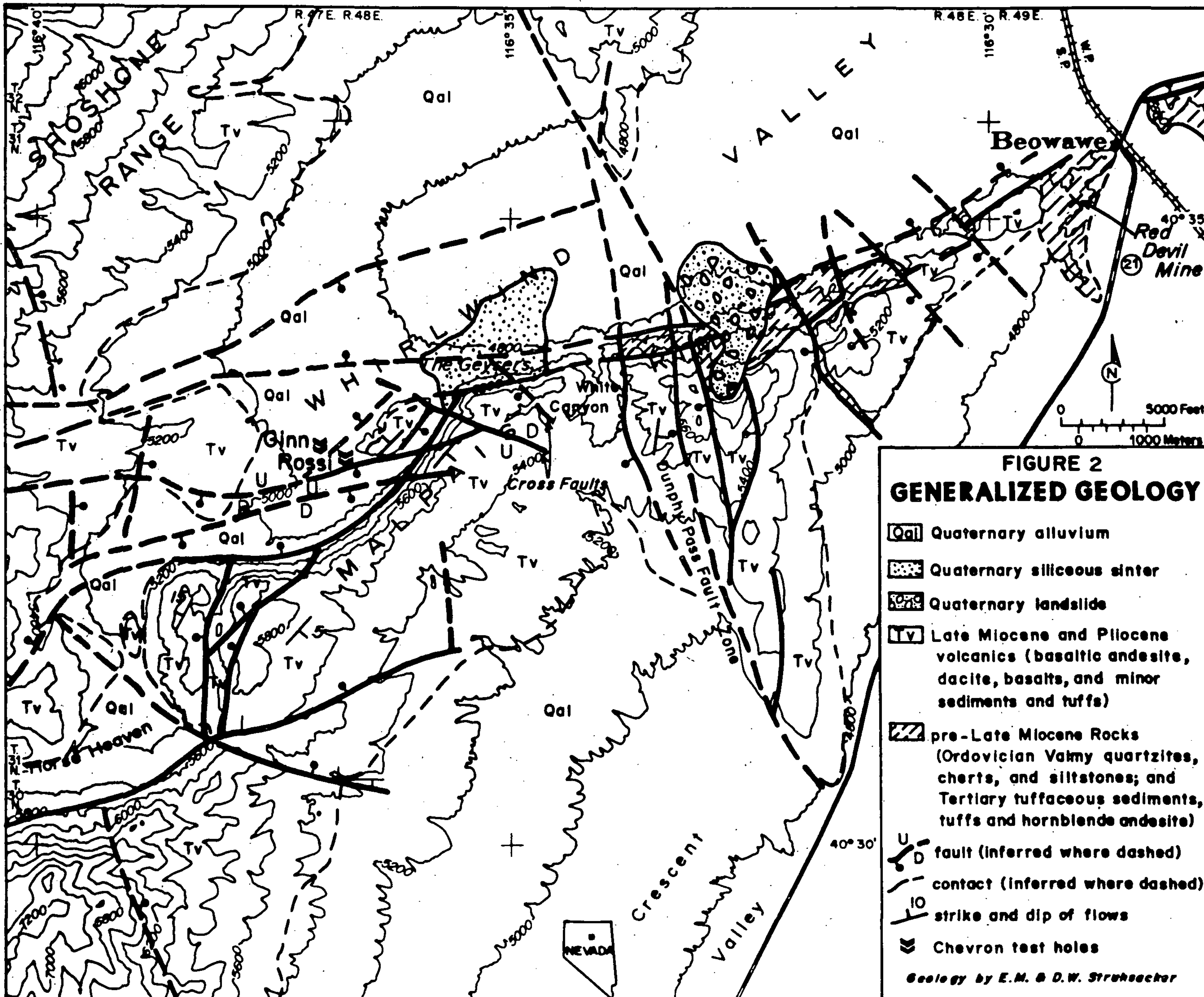

FIGURE 2
GENERALIZED GEOLOGY

the margin of the graben juxtapose Ordovician Valmy eugeosynclinal meta-sediments on the east and 1200+ m of Miocene pyroxene dacite flows and tuffaceous rocks on the west. Silicified fault breccia and country rock at the intersection of the Dunphy Pass fault zone and the east-west fault at the base of the Malpais are surrounded by zones of pervasive argillization. These signs of hydrothermal alteration extend up White Canyon into the Malpais.

Geophysical Setting

The earliest indication of a conductive anomaly in the Malpais was given by two bipole-dipole apparent resistivity maps (Wollenberg and others, 1975). Figure 3 is their map for the transmitter located in the Whirlwind Valley. The concern that the bipole-dipole method fails to contribute useful information can be critically evaluated through comparisons of these data and theoretical data from simple models generated by the integral equation numerical simulator developed by Hohmann (1975).

A circular area of low resistivity (<30 ohm-m) at The Geysers is flanked on the west by a finger of higher resistivity (>50 ohm-m) that wraps around the circular low (Figure 3). A companion high-resistivity pattern occurs east of White Canyon. This combination of a local low surrounded by higher values can be produced by a shallow conductive body (Hohmann and Jiracek, 1979) in a layered, low-over-high resistivity earth model (Zohdy, 1978).

Numerical simulations restricting the conductive body to the area of The Geysers fail to reproduce the low values observed on the Malpais on the finger of low resistivities at the mouth of White Canyon in the Whirlwind Valley. To

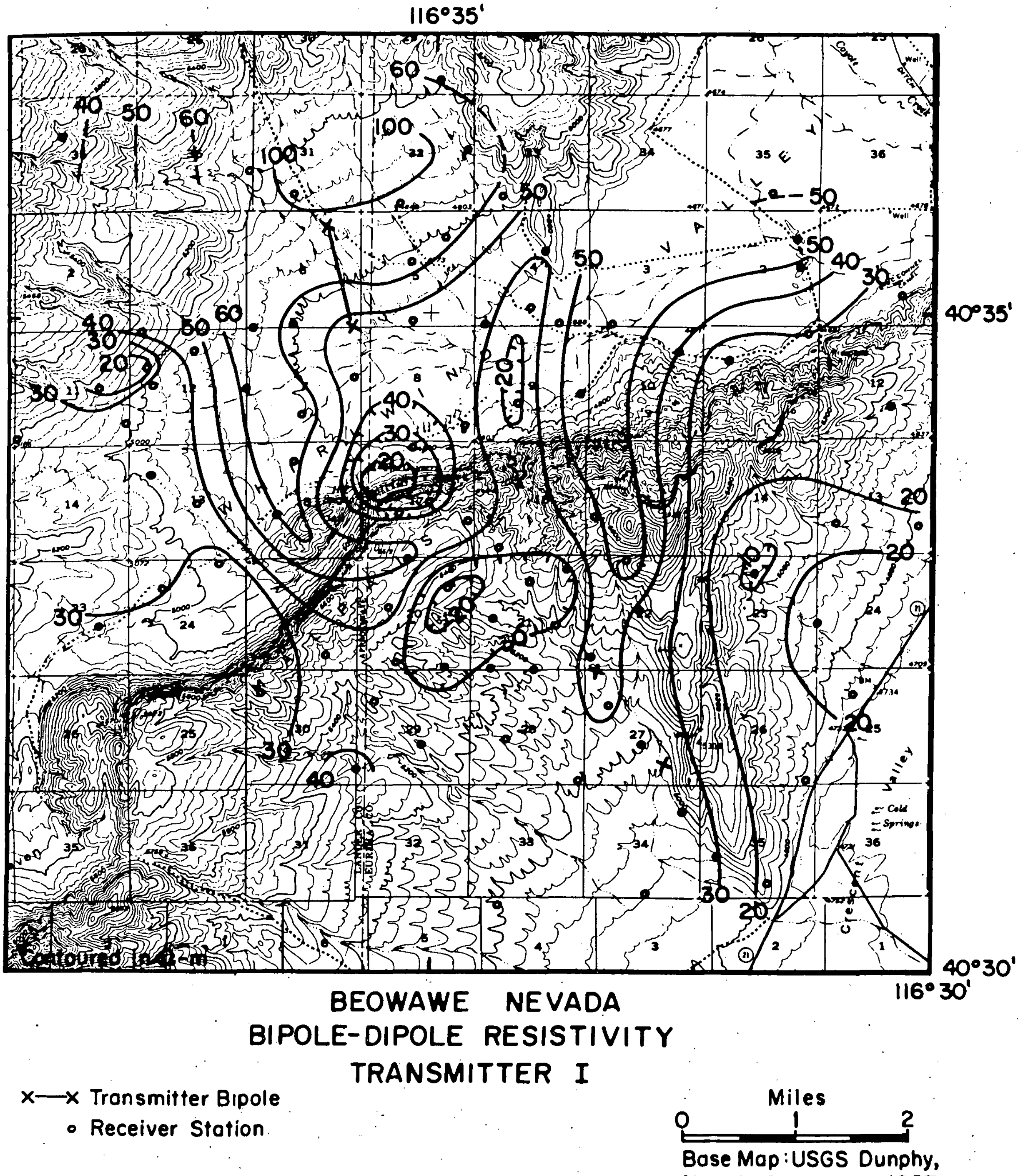

XBB 743-1632

FIGURE 3 BIPOLE-DIPOLE APPARENT RESISTIVITY MAP, WHIRLWIND VALLEY TRANSMITTER (FROM WOLLENBERG AND OTHERS, 1975, LAWRENCE BERKELEY LABORATORY) simulate all the observed patterns, the conductor must extend southeast of The Geysers below the Malpais and down White Canyon into the Whirlwind Valley. Figure 4 is a plan view of the 3D numerical model used to generate the theoretical data shown in Figure 5. The conductor has an intrinsic resistivity of 10 ohm-m and is surrounded by a 60 ohm-m half space. No attempt has been made to account for the effects of layering or to duplicate the amplitudes of the observed patterns or the effect of the topography of the Malpais (Zoback, 1979). A comparison between Figures 3 and 5 reveal that the theoretical data mimic the observed patterns fairly well. The model of Figure 4 is certainly non-unique but appears to be an adequate simulation of the anomaly detected by the bipole-dipole experiment.

The bipole-dipole data suggest that a deep, conductive body associated with the geothermal resource at The Geysers extends southeast below the Malpais. Even though the depth, depth extent, and lateral boundaries of the anomaly are poorly delimited, the method provides a reconnaissance view that can be used to site more precise and costly exploration methods. As noted by Wollenberg and others (1975), dipole-dipole resistivity or some other profiling technique is required to obtain a better understanding of the resistivity distribution below the Malpais.

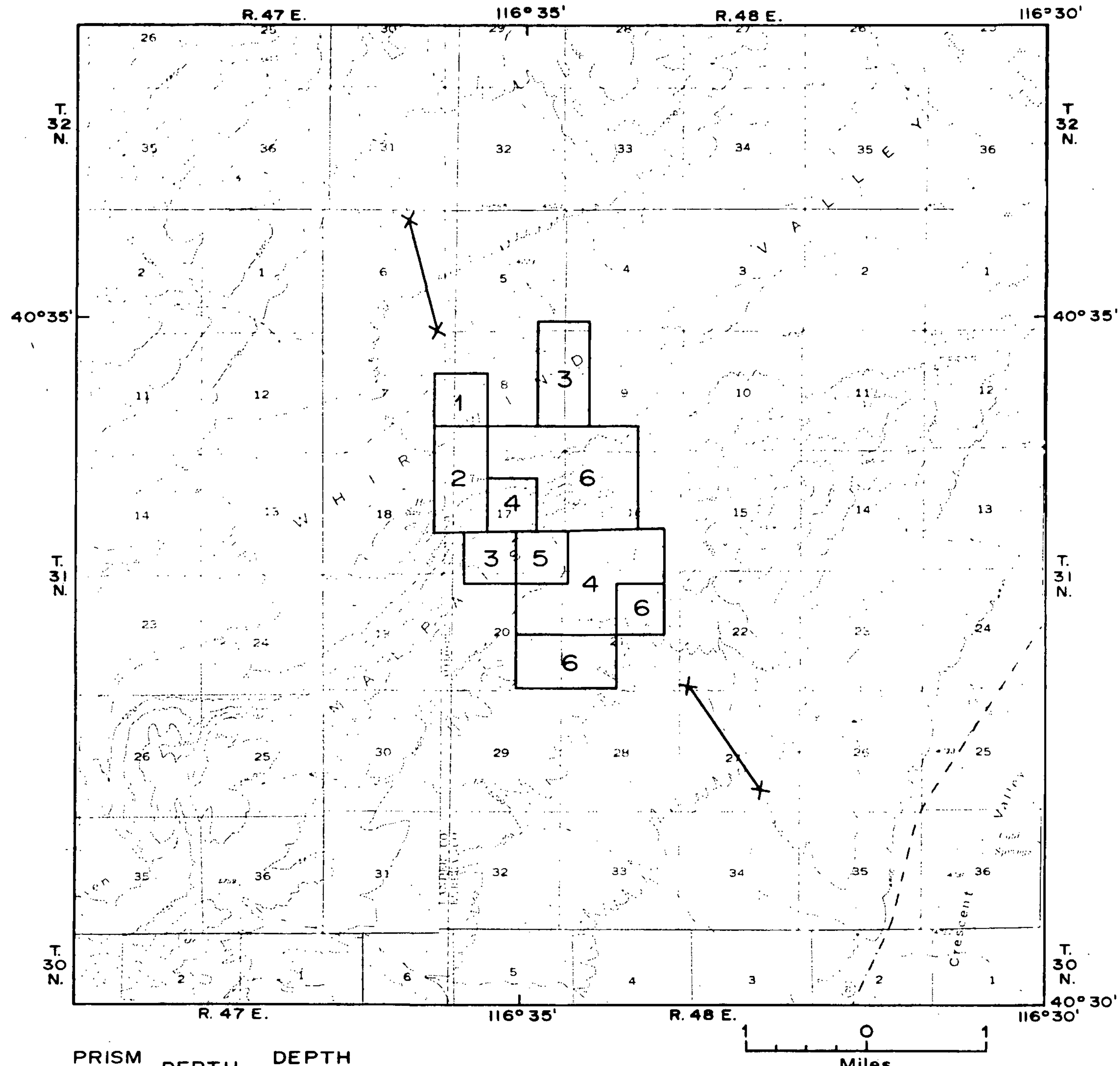

PRISM NO.	DEPTH	DEPTH EXTENT
1	0.1	2.0
2	0.1	3.0
3	0.2	1.0
4	0.2	2.0
5	0.2	3.0
6	0.5	1.0

(1 unit = 725 m)

X———X Bipole Transmitter

Background Resistivity 60 ohm-m

Anomaly Resistivity 10 ohm-m

FIGURE 4 THREE-DIMENSIONAL INTERPRETATION MODEL FOR LAWRENCE BERKELEY LABORATORY BIPOLE-DIPOLE DATA.

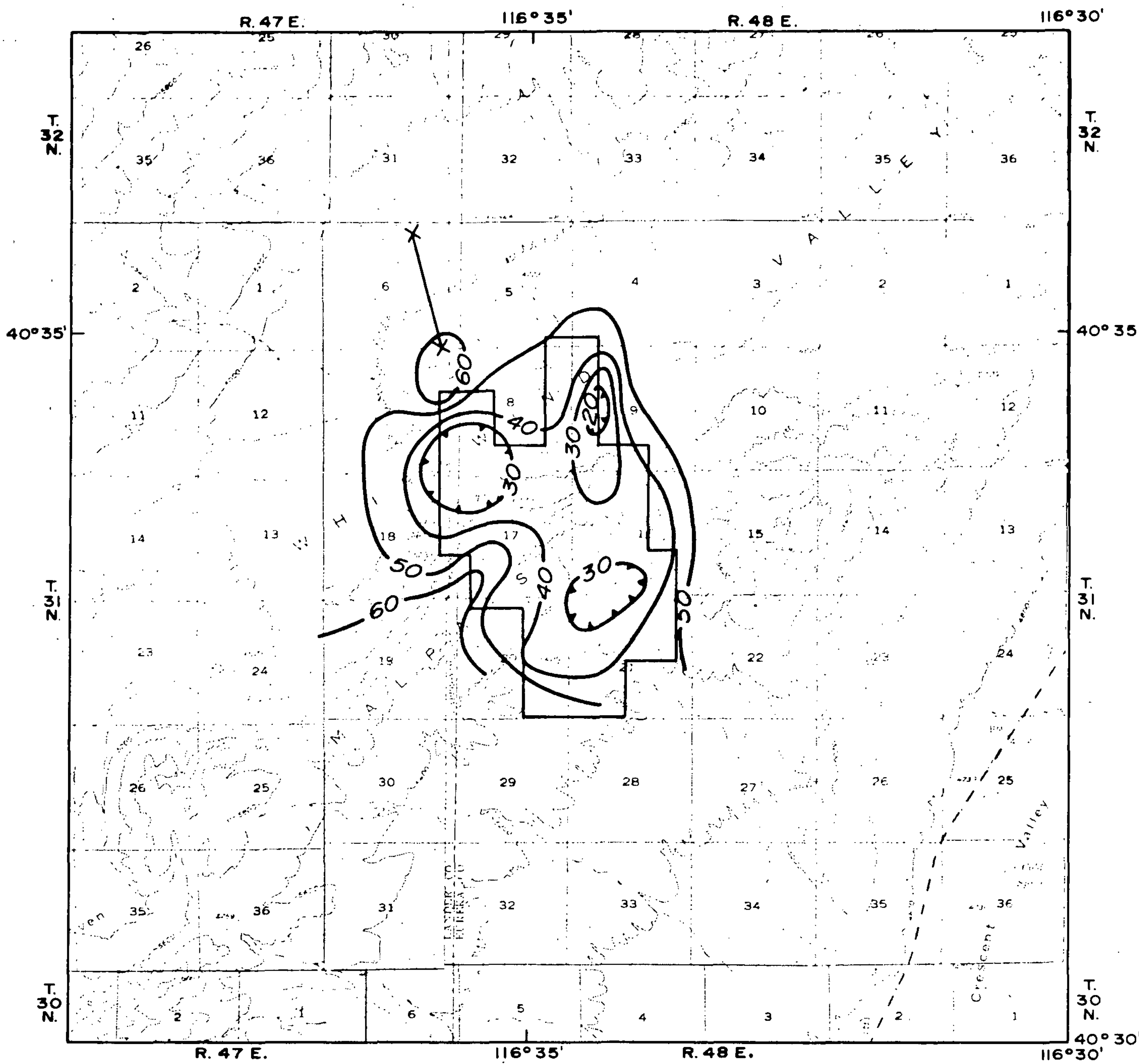

Whirlwind Valley Transmitter

Contours in ohm-m

1 0 1

Miles

FIGURE 5 THEORETICAL BIPOLE-DIPOLE APPARENT RESISTIVITY MAP.

DIPOLE-DIPOLE RESISTIVITY

Description of Surveys

Four north-south dipole-dipole profiles with 2000-foot dipoles cross the Malpais along section lines (Figure 6). These data were recorded by McPhar Geophysics in July and November 1974 for Chevron Resources Co. and are part of the Department of Energy/Division of Geothermal Energy's open-file data package from Beowawe (Earth Science Laboratory, 1979). Numerical models of these data were discussed by Smith (1979) who suggests that a conductive (<15 ohm-m) body may lie below the Malpais. The data do not extend far enough to the south to define the inferred conductor.

To determine the resistivity distribution below the Malpais, three additional dipole-dipole profiles were recorded by JCW, Inc. for the Earth Science Laboratory in April, 1980 (Figure 6). The profiles cross the Dunphy Pass fault zone and are approximately perpendicular to it. These data are presented here as part of the open-file information sponsored by the Department of Energy/Division of Geothermal Energy.

The current source for the JCW, Inc. survey was a Scintrex Model IPC-7, 15 kw square-wave transmitter that output an average current of 12.0 ±0.5 amps peak. Induced voltage was measured to ±0.1 mv with non-polarizing porous plots, a Scintrex Model IPR-10 digital time-domain IP receiver, and a Scintrex Model IPR-8A receiver in conjunction with a Hewlett Packard Model 7155B strip-chart recorder. Dipole lengths for Lines MR 1 and MR 2 are 2000 feet; for Line MR 3, 1000 feet.

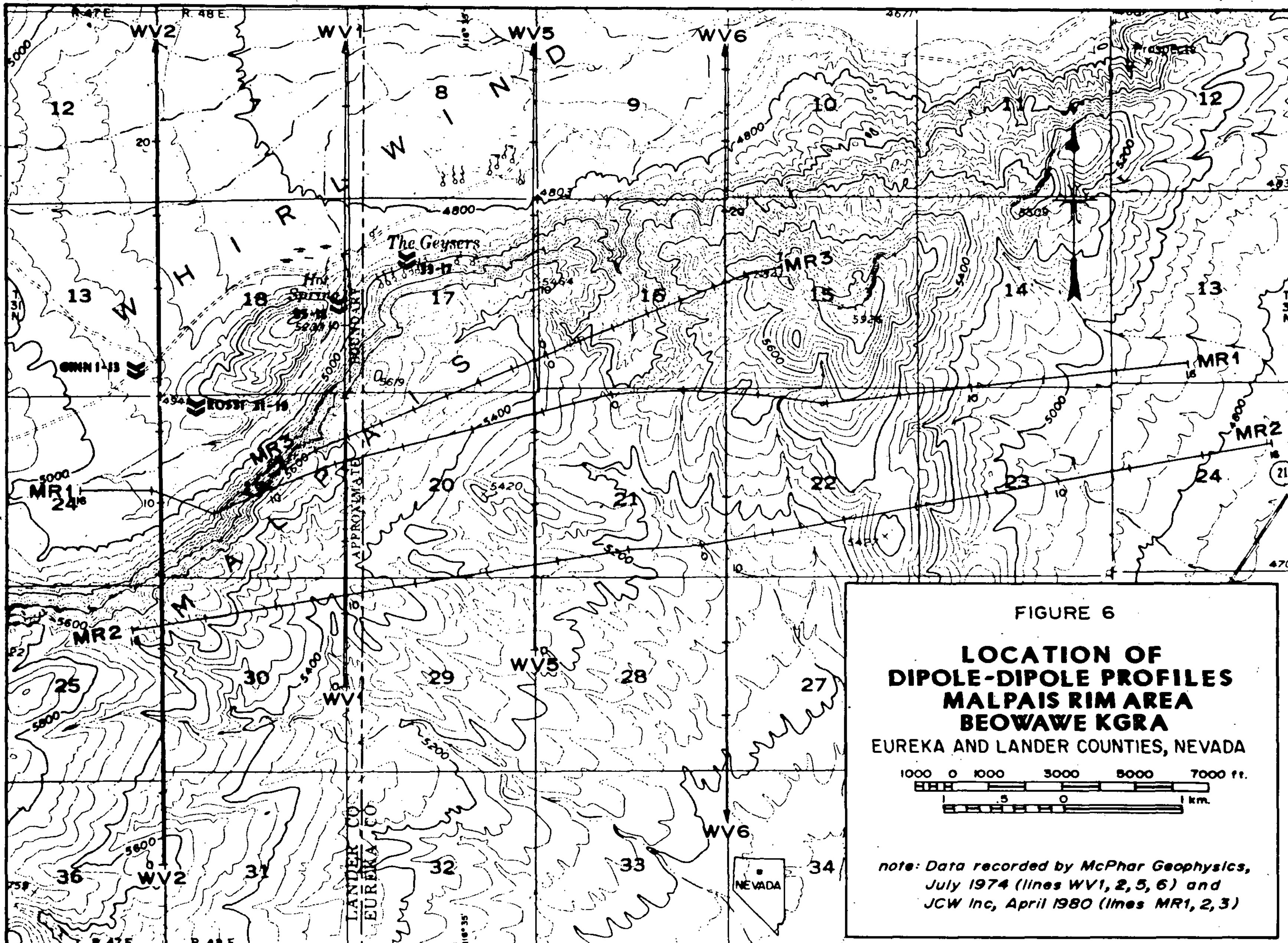

FIGURE 6

LOCATION OF DIPOLE-DIPOLE PROFILES MALPAIS RIM AREA BEOWAWE KGRA

EUREKA AND LANDER COUNTIES, NEVADA

note: Data recorded by McPhar Geophysics, July 1974 (lines WV1, 2, 5, 6) and JCW Inc, April 1980 (lines MR1, 2, 3)

A 2D finite-element algorithm developed by Rijo (1977) and modified by the Earth Science Laboratory (Killpack and Hohmann, 1979) was used to produce models of the resistivity distribution along the three profiles (Figures A1-A3). Figures 7-9 present the interpreted resistivity profiles with the observed apparent resistivities and Figure 10 presents the interpreted resistivity distribution at an elevation of 3000 feet. The results from the north-south profiles modeled by Smith (1979) are less well constrained but are included in Figure 10. Agreement among the models is generally good where the profiles intersect. Where discrepancies occur, greater weight has been given to the east-west data which are more nearly perpendicular to the Dunphy Pass fault zone.

Interpretation

The interpreted resistivity sections, Figures 7-9, contain intrinsic resistivities that range from 10 to 200 ohm-m. Lateral contrasts in resistivity are more pronounced than layering. The scale for Figures 7 and 8 (2000-ft dipoles) is twice that of Figure 9 (1000-ft dipoles).

To avoid disturbing fledgling eagles in their nests, Line MR 1 was not completed as a straight line where it crosses the cliff southwest of The Geysers. As a result, the westernmost two dipoles produce low resistivities (10 and 20 ohm-m, Figure A-1) that are partly due to their non-linear orientation. The low resistivities computed at the west end of Line MR 1 are considered to be unreliable representations of the resistivity distribution of the Whirlwind Valley and are omitted from the interpreted model, Figure 7. The mesh geometry for all three models attempts to simulate the topography of

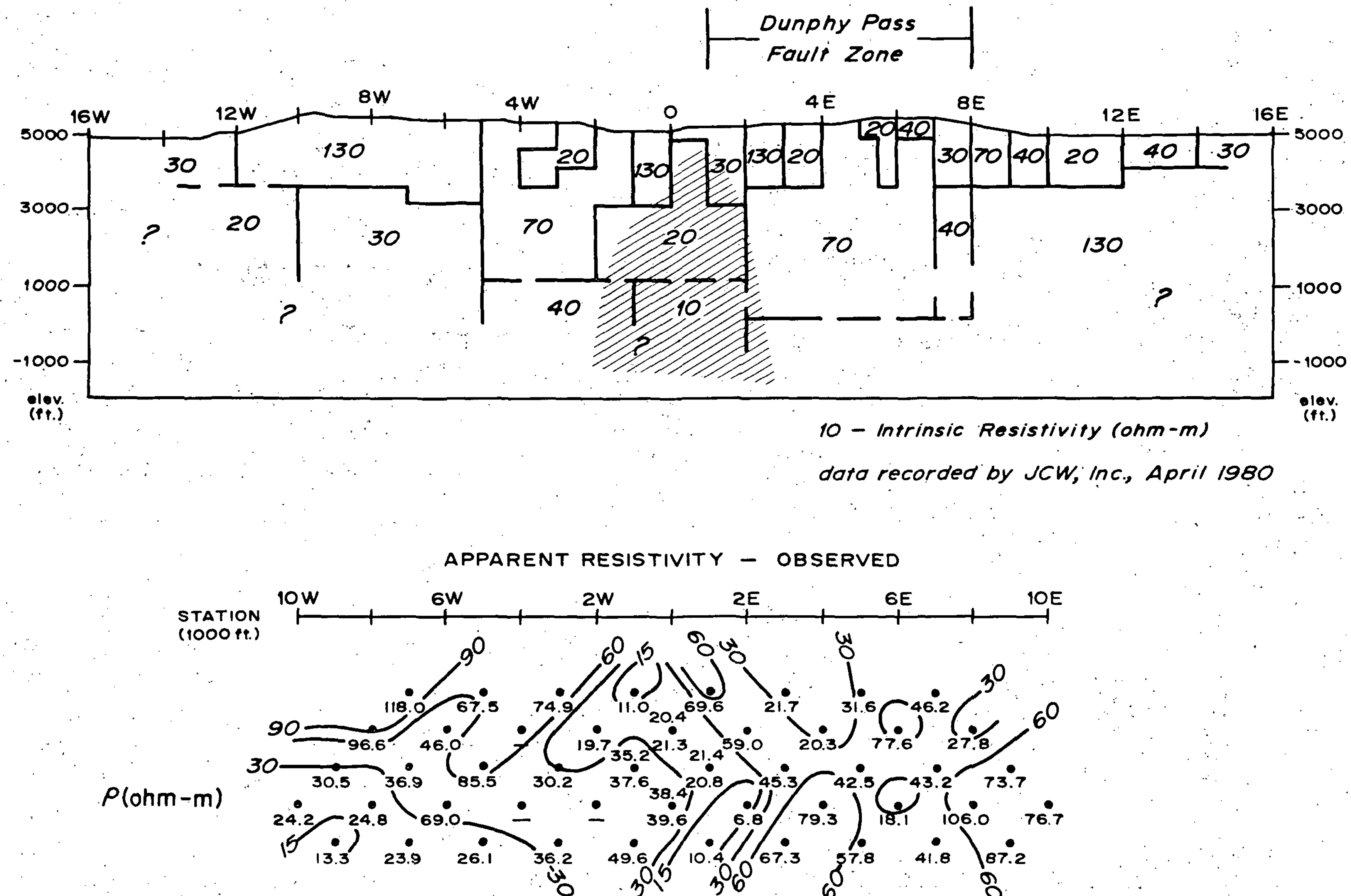

FIGURE 7 INTERPRETED RESISTIVITY SECTION AND OBSERVED APPARENT RESISTIVITY
LINE MR1 – MALPAIS AREA
BEOWAWE KGRA
EUREKA AND LANDER COUNTIES, NEVADA
Scale 1:48,000

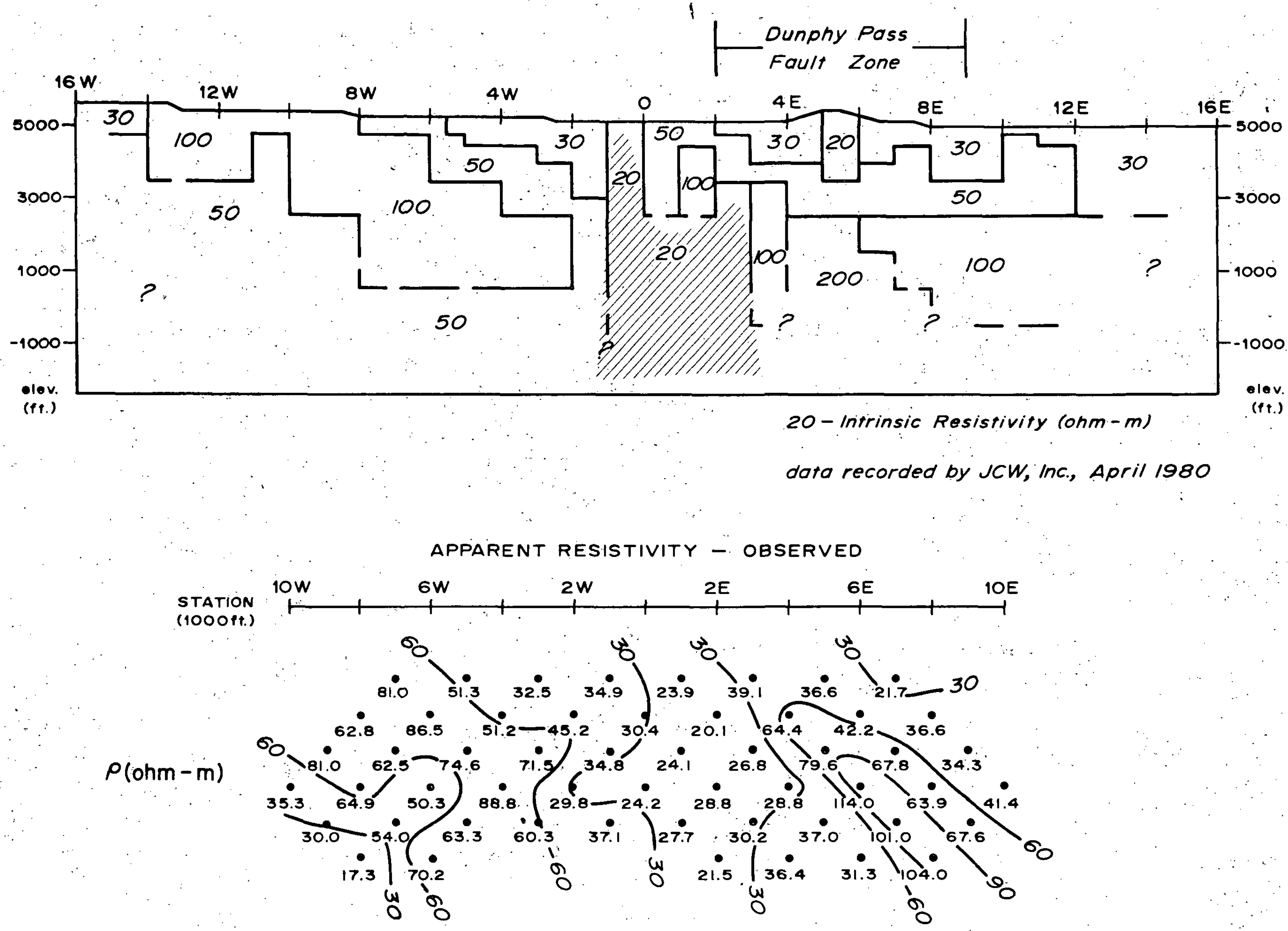

FIGURE 8 INTERPRETED RESISTIVITY SECTION AND OBSERVED APPARENT RESISTIVITY
LINE MR2 — MALPAIS AREA
BEOWAWE KGRA
EUREKA AND LANDER COUNTIES, NEVADA
Scale 1:48,000

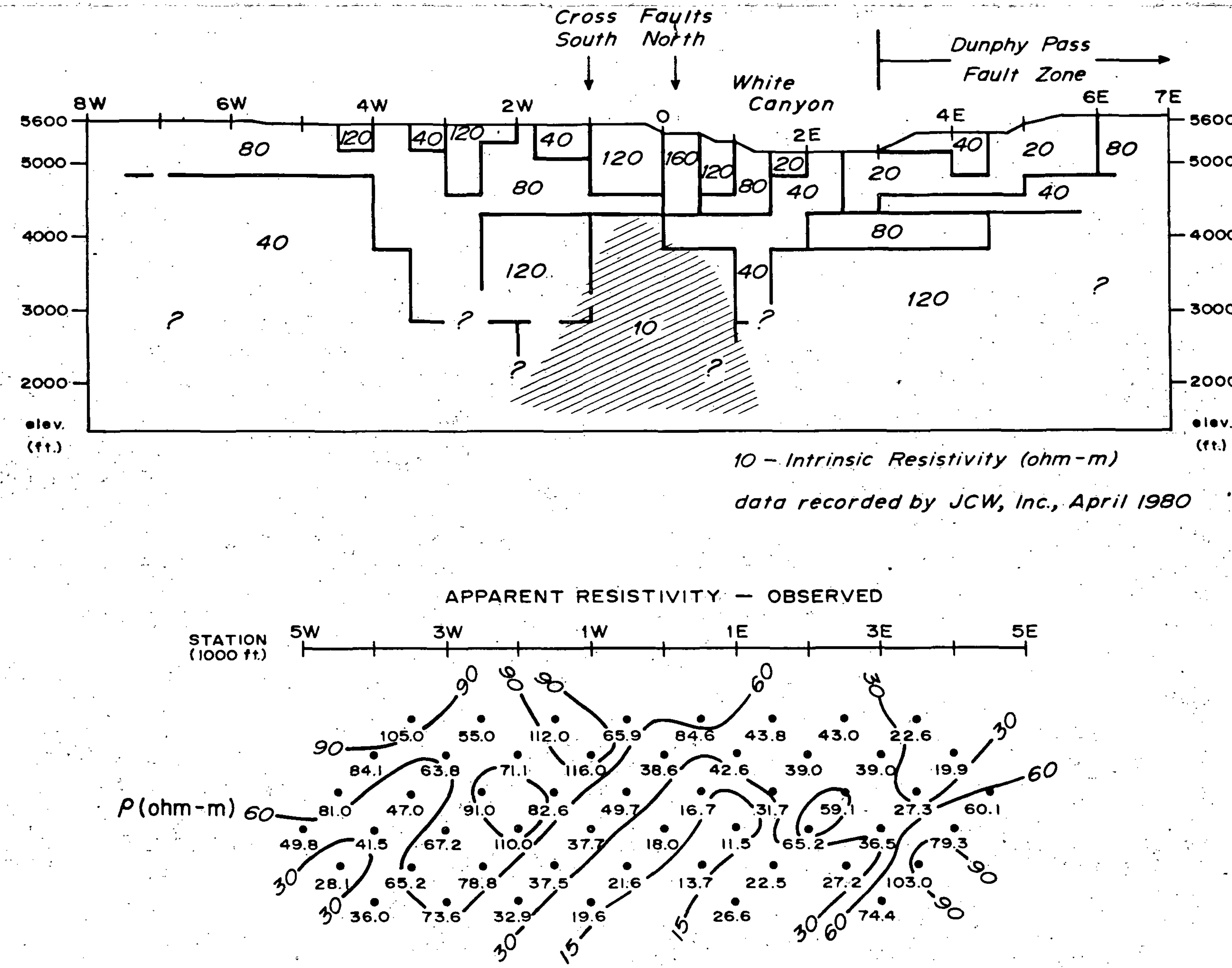

FIGURE 9 INTERPRETED RESISTIVITY SECTION AND OBSERVED APPARENT RESISTIVITY
LINE MR3 — MALPAIS AREA
BEOWAWE KGRA
EUREKA AND LANDER COUNTIES, NEVADA
Scale 1:24,000

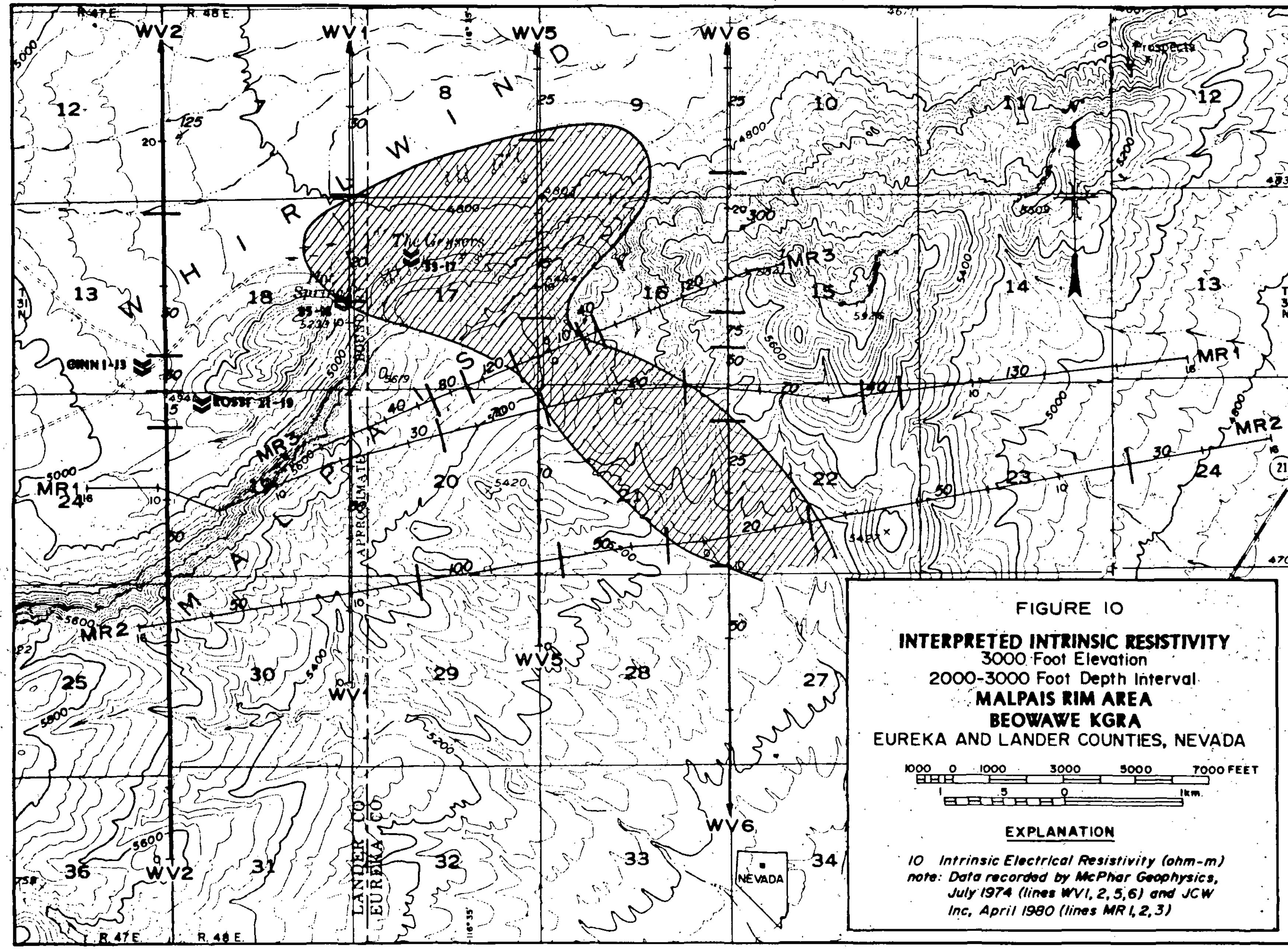

FIGURE 10

INTERPRETED INTRINSIC RESISTIVITY
3000 Foot Elevation
2000-3000 Foot Depth Interval
MALPAIS RIM AREA
BEOWAWE KGRA
EUREKA AND LANDER COUNTIES, NEVADA

1000 0 1000 3000 5000 7000 FEET
1 .5 0 1km.

EXPLANATION

10 Intrinsic Electrical Resistivity (ohm-m)
note: Data recorded by McPhar Geophysics, July 1974 (lines WV1, 2, 5, 6) and JCW Inc, April 1980 (lines MR 1, 2, 3)

the Malpais; topographic effects were found to be as large as ±25%.

Line MR 2 (Figure 8) is the profile furthest from The Geysers and presumably the least influenced by the hydrothermal system. Its interpreted resistivity distribution is the least complex. Even so, it defines a deep-seated conductive anomaly west of the mapped location of the Dunphy Pass fault zone. This body is the salient feature common to all three sections and was detected along Line WV 5 and Line WV 6 (Figure 10). The models suggest that this body has resistivities as low as 10 ohm-m, a maximum east-west width of 1250 m (4000 ft), and extends to depths of at least 2 km. Its eastern boundary is invariably defined by large blocks with resistivities greater than 50 ohm-m within the Dunphy Pass fault zone. Contrasts in resistivities across its western boundary are generally less pronounced.

The conductor is shown to reach the surface along Line MR 1 (Figure 7) between stations 0 and 2W. The 30 ohm-m body at the surface between these stations probably represents the tuff unit that crops out at the head of White Canyon; most of the bodies with resistivities of 40 ohm-m or less at the surface along all three profiles correlate with outcrops of tuffaceous sediment. Even though the conductor appears to reach the surface along Line MR 1, the tuff at the head of White Canyon is too thin to be the source of the anomaly at depth. Other tuff units that do not crop out may produce the deep-seated low-resistivity zone.

The 1000-ft dipoles of Line MR 3 provide more near-surface detail than the 2000-ft dipoles of Lines MR 1 and 2 and indicate that the conductor does not reach the surface (Figure 9). Instead, the 10 ohm-m anomaly occurs at a depth of approximately 375 m (1200 ft) between stations 1W and 0, west of White Canyon and the exposures of tuffaceous sediment. It underlies a particularly resistive (120-160 ohm-m) section that may be related to outcrops of the basalt that is the youngest volcanic unit in the Beowawe area. The 120 ohm-m body at depth below stations 2.5W and 1W may be a local 3D body or it may reflect a major lithologic break within the volcanic pile.

The Malpais conductor may reflect argillization caused by a defunct episode of hydrothermal activity or, possibly, a zone that is still connected in some way to the active hydrothermal system at The Geysers. While it is unlikely, the anomaly might also be caused by conductive Ordovician shales at a shallow depth within the Miocene graben. These possibilities could be tested with information from 500 m thermal gradient holes.

Below the Whirlwind Valley, the volcanic rocks have resistivities greater than 50 ohm-m and the underlying Ordovician meta-sediments resistivities less than 30 ohm-m (Smith, 1979). A similar contrast is not seen across the Dunphy Pass fault zone. Instead, the Ordovician rocks on the east have resistivities greater than 50 ohm-m. Several factors could contribute to the high resistivities east of the Dunphy Pass fault zone: primary lithologic facies changes, lack of saturation by hydrothermal fluids, or secondary hydrothermal silicification. The collection and analysis of chip samples from thermal gradient holes on the Malpais may reveal why the meta-sediments have much higher resistivities below the Malpais than they do below the Whirlwind Valley.

CONCLUSIONS

Bipole-dipole data point to a poorly resolved anomaly below the Malpais. Dipole-dipole data define a conductor 1200 m wide at a depth of 300-400 m with an undetermined depth extent.

Both the conductive anomaly and The Geysers are confined between the North and South Cross-Faults of Osterling (1962) (Figure 10). The anomaly extends southeast beyond the exposures of the cross-faults, intersects the Dunphy Pass fault zone within section 22, T31N, R48E, and may possibly connect The Geysers to the deep-seated faults at the margin of a Miocene graben. Thermal gradient data may resolve whether this conductor is associated with a source of heat.

ACKNOWLEDGEMENTS

The bipole-dipole data were supplied by Dr. N. E. Goldstein, Lawrence Berkeley Laboratories. The dipole-dipole data recording, modeling, and interpretation were funded by contract DE-AC07-80ID12079 as part of the Department of Energy/Division of Geothermal Energy's Industry Coupled Program. Connie Wiscombe typed the manuscript and Connie Pixton drafted the figures.

REFERENCES

Earth Science Laboratory, 1979, Chevron Resources Co., data on Beowawe, Nevada: Open-file release of March, 1979, Salt Lake City.

Earth Science Laboratory, in preparation, Case study of the Beowawe area, north-central Nevada.

Hohmann, G. W., 1975, Three-dimensional induced polarization and electromagnetic modeling: Geophysics, v. 40, p. 309-324.

Hohmann, G. W., and Jiracek, G. R., 1979, Bipole-dipole interpreation with three-dimensional models (including a field study of Las Alturas, New Mexico): Universty of Utah Research Institute, Earth Science Laboratory Rept. 20, 48 p.

Killpack, T. J., and Hohmann, G. W., 1979, Interactive dipole-dipole resistivity and IP modeling of arbitrary two-dimensional structures (IP2D user's guide and documentation): University of Utah Research Institute, Earth Science Laboratory Rept. 15, 107 p.

Osterling, W. A., 1962, Geothermal power potential of northern Nevada: text of paper presented at the 1962 Pacific Southwest Mineral Industry Conference of the A.I.M.E.

Rijo, Luiz, 1977, Modeling of electrical and electromagnetic data: Ph.D. disseration, Univ. of Utah, Dept. of Geology and Geophysics, 242 p.

Smith, Christian, 1979, Interpretation of electrical resistivity and shallow seismic reflection profiles, Whirlwind Valley and Horse Heaven areas, Beowawe KGRA, Nevada: Univ. of Utah Research Institute, Earth Science Laboratory Rept. 25, 43 p.

Struhsacker, E. M., 1980, Geology of the Beowawe geothermal area, Eureka and Lander Counties, Nevada: Univ. of Utah Research Institute, Earth Science Laboratory Rept. 37.

Wollenberg, A. A., Asara, F., Bowman, H., McEvilley, T., Morrison, F., and Witherspoon, P., 1975, Geothermal energy resource assessment: Lawrence Berkeley Laboratory, Energy and Environment Division, UCID 3762, 92 p.

Zoback, M. L. C., 1978, Mid-Miocene rifting in north-central Nevada: A detailed study of late-Cenozoic deformation in the northern Basin and Range: Ph.D. dissertation, Stanford Univ., 247 p.

Zoback, M. L. C., 1979, A geological and geophysical investigation of the Beowawe geothermal area, north-central Nevada: Stanford University Publications, Geological Sciences, v. XVI, 79 p.

Zohdy, A. A. R., 1978, Total field resistivity mapping and sounding over horizontally layered media: Geophysics, v. 43, no. 4, p. 748-766.

APPENDIX

Pages 23-25 document all final models. The computed resistivity values are contoured in the same manner as the observed data (Figure 7-9) to facilitate comparison. The resistivities and mode thickness used in the numerical models are indicated for each model. Unless otherwise indicated, all node widths are 0.25 dipole lengths.

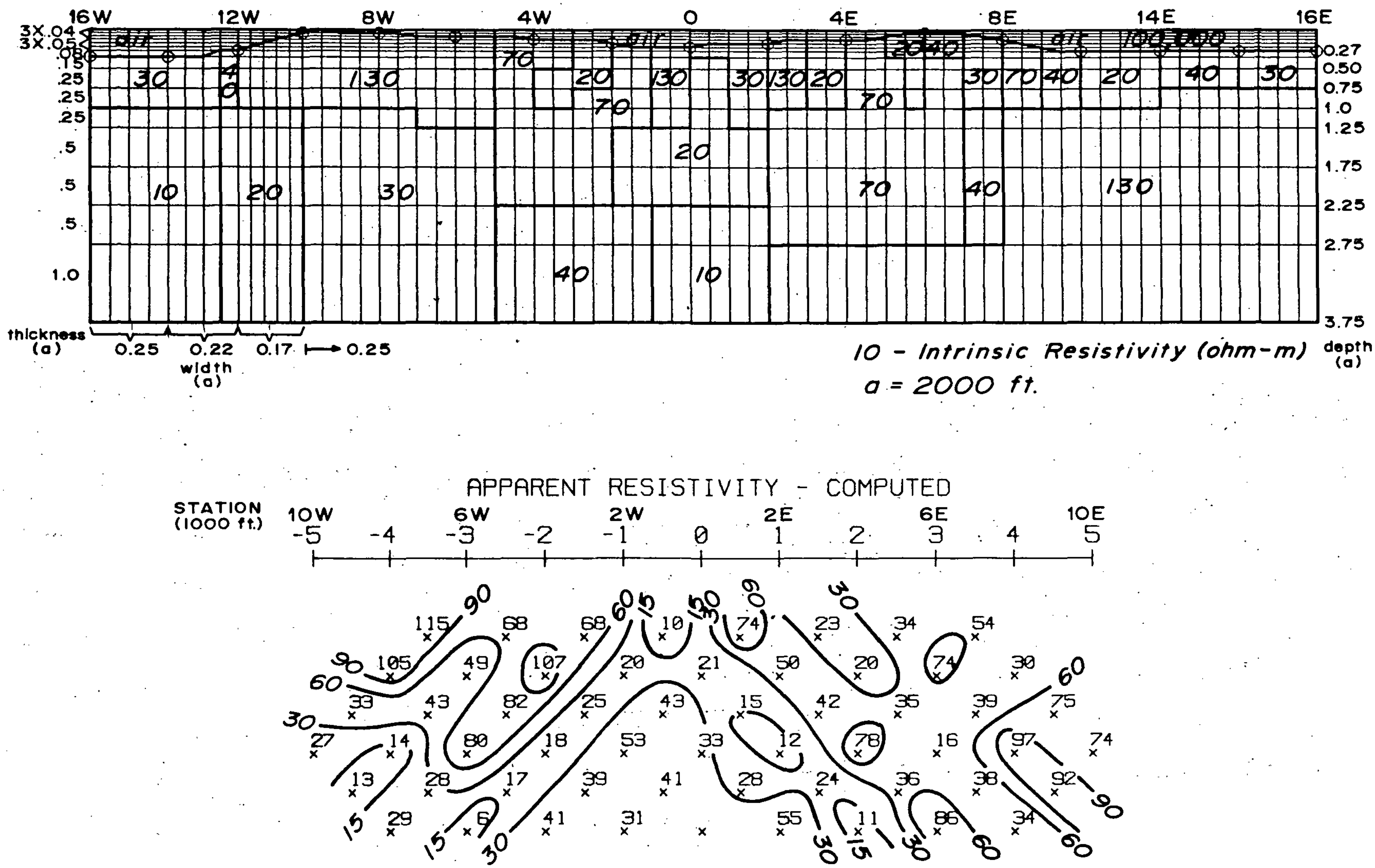

FIGURE A-1 COMPUTED MODEL, LINE MR1, MALPAIS AREA, ITERATION 8

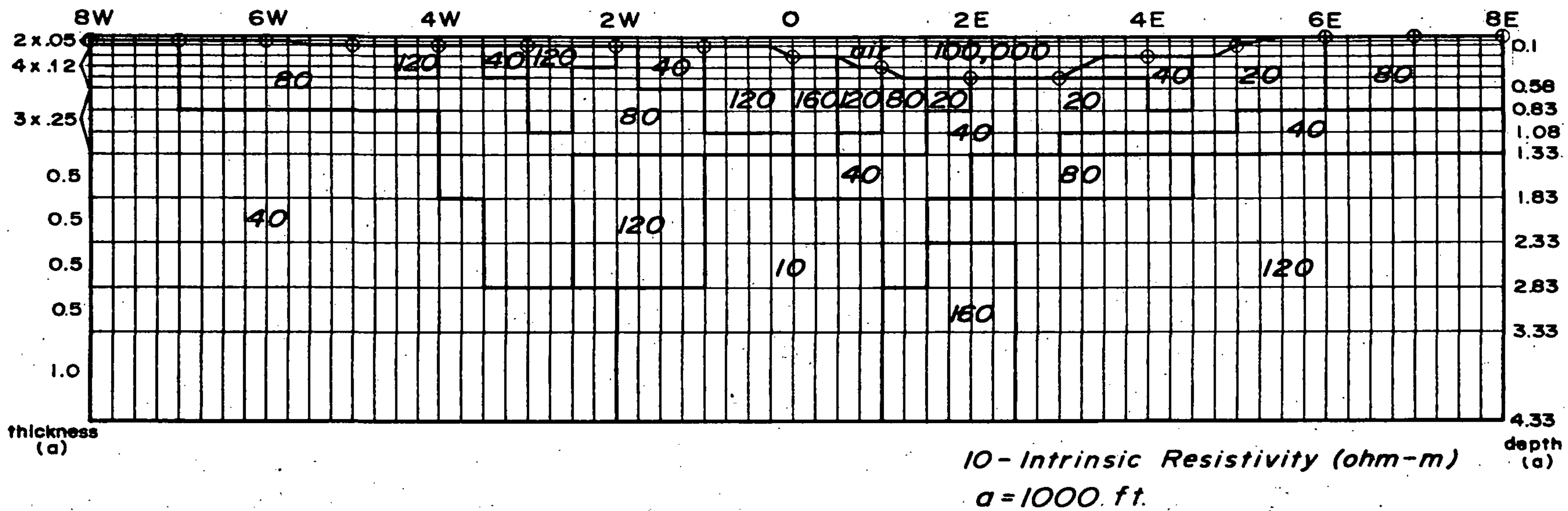

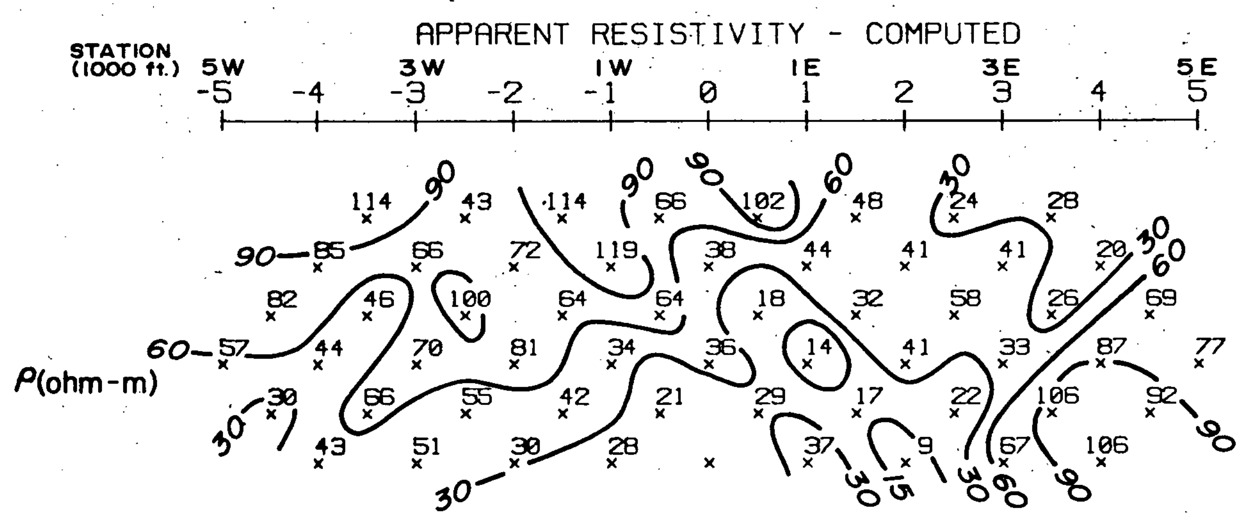

FIGURE A-3 COMPUTED MODEL, LINE MR3, MALPAIS AREA, ITERATION 6

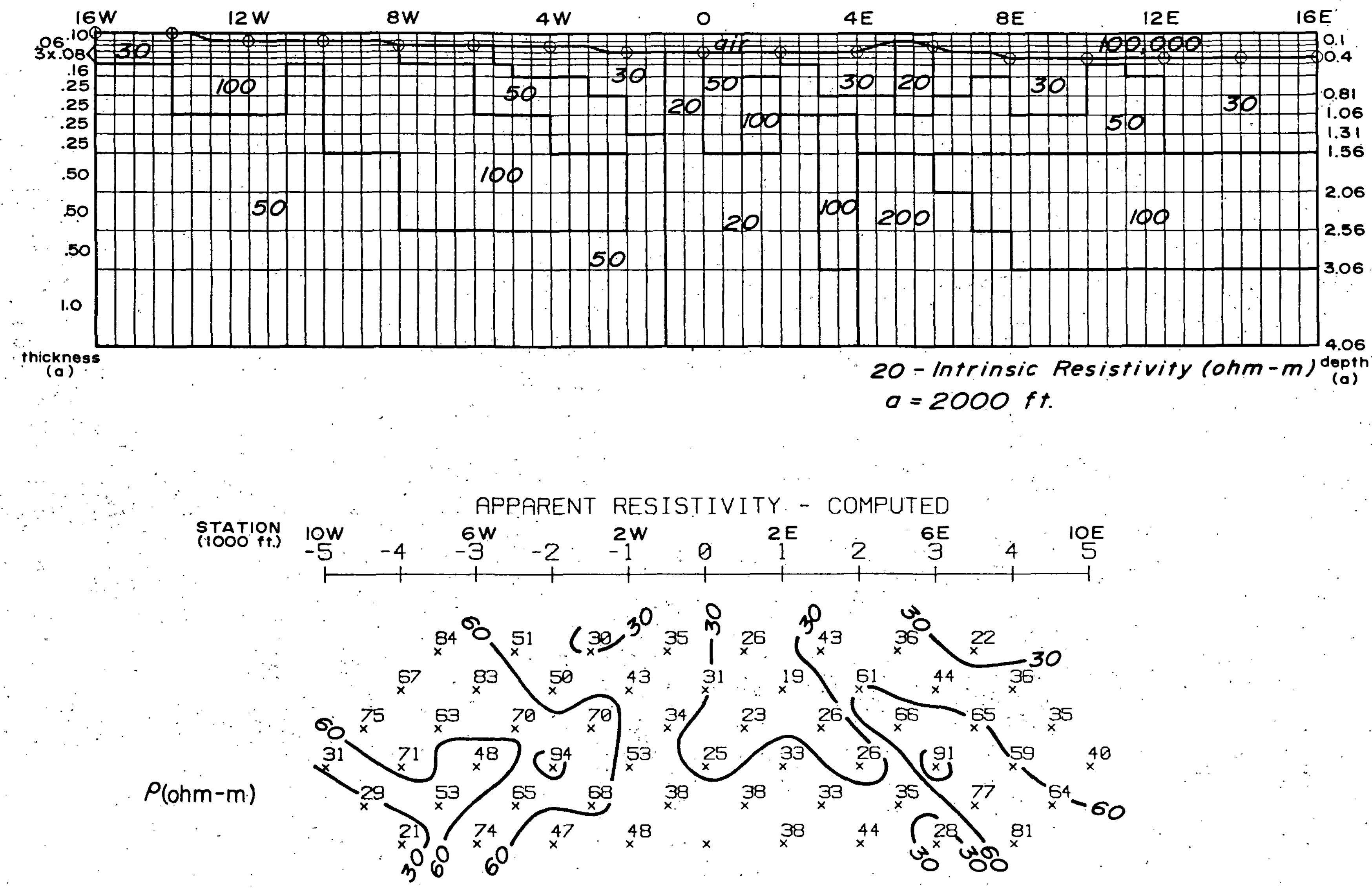

FIGURE A-2 COMPUTED MODEL, LINE MR2, MALPAIS AREA, ITERATION 5